

## Quantitative detection of chlorophyll in cyanobacterial blooms by satellite remote sensing

Tiit Kutser<sup>1</sup>

Department of Limnology, University of Uppsala, Norbyvägen 20, SE-752 36, Uppsala, Sweden

### Abstract

The extent of cyanobacterial blooms has been mapped using different satellite sensors from weather satellites to synthetic aperture radars. Quantitative detection of chlorophyll in cyanobacterial blooms by remote sensing, however, has been less successful. The first civilian hyperspectral sensor in space, Hyperion, acquired an image of cyanobacterial bloom in the western part of the Gulf of Finland on 14 July 2002. A chlorophyll concentration map was produced from this image using a spectral library that was created by running a bio-optical model with variable concentrations of chlorophyll. The results show that chlorophyll concentrations in the bloom area were much higher than reported by conventional water-monitoring programs, ships-of-opportunity, and satellite measurements. The reason why both in situ and satellite methods underestimate the amount of phytoplankton during cyanobacterial blooms is vertical and horizontal distribution of cyanobacteria, because cyanobacteria can regulate their buoyancy and are not uniformly distributed within the top mixed layer of water column in calm weather conditions. Aggregations of cyanobacteria form dense subsurface blooms and surface scums during extensive blooms. This study demonstrates that it is difficult to collect representative water samples from research vessels using standard methods because ships and water samplers destroy the natural distribution of cyanobacteria in the sampling process. Flow-through systems take water samples from the depths at which the concentration of cyanobacteria is not correlated with the amount of phytoplankton that remote sensing instruments detect. The chlorophyll estimation accuracy in cyanobacterial blooms by many satellites is limited because of spatial resolution, as significant changes in chlorophyll concentration occur even at a smaller spatial scale than 30 m.

It has been shown (Rantajärvi et al. 1998) that spatial and temporal frequencies of conventional water-sampling programs are not adequate to report changes in phytoplankton biomass, especially during bloom conditions, when spatial and temporal variability in phytoplankton density is particularly high. Reliable quantitative monitoring of cyanobacterial blooms is even more complicated. This is caused by the nature of cyanobacterial blooms, in which the algae, capable of regulating their buoyancy, can be located in the top layer of water or at the water surface instead of being uniformly mixed in the water column (Paerl and Ustach 1982; Sellner 1997). Knowledge about the amount of phytoplankton has important implications for primary production and carbon cycle models as well as for monitoring the state of water bodies. A large uncertainty in detection of the amount of chlorophyll occurs during cyanobacterial blooms. Reliable mapping of the amount of cyanobacteria is especially important in the case of the Baltic Sea, where the cyanobacterial blooms may cover an area of more than 100,000 km<sup>2</sup> (Kahru 1997), affecting recreation, ecosystem integrity, and human and animal health.

The use of unattended flow-through systems on ships-of-opportunity (Leppänen et al. 1995; Rantajärvi et al. 1998) and airborne (Dekker et al. 1992; Jupp et al. 1994) and sat-

ellite remote sensing (Kahru et al. 1993, 2000; Kahru 1997) have been recommended to provide more reliable information about the extent of the cyanobacterial blooms than the conventional monitoring programs can provide. However, standard algorithms developed for MODIS or SeaWiFS overestimate chlorophyll concentrations in the Baltic Sea by 150–200% even in nonbloom conditions (Darecki and Stramski 2004).

Some success in the quantitative mapping of cyanobacteria has been achieved using airborne remote sensing (Dekker et al. 1992). In this work the amount of cyanobacteria was detected through the amount of pigments unique to cyanobacteria—cyanophycocerythrin (CPE) and cyanophycocyanin (CPC). For example, a band ratio 624/648 nm was recommended to estimate concentration of CPC from CASI data. In Dekker (1993), a more sophisticated CPC absorption algorithm was developed and applied to hyperspectral airborne imagery of lakes in The Netherlands. The algorithm was parameterized using an analytical model using specific inherent optical properties and a CPC-specific absorption coefficient. Hyperion (and MERIS) have sufficient spectral resolution to enable mapping of phycocyanin from space. The spatial resolution of Hyperion should also be adequate for that purpose, as Vincent et al. (2004) have shown that Landsat, which has similar spatial resolution, can be used for mapping of phycocyanin (despite the fact that the phycocyanin absorption feature is located between Landsat bands). The problem is that CPE and CPC are not routinely measured from water samples, and there is no information available about the CPE and CPC concentrations in the Baltic Sea cyanobacteria. Therefore, it would be desirable to map the amount of cyanobacteria through chlorophyll concentration, as the concentration of chlorophyll *a* is often used as a proxy of algal biomass in water.

<sup>1</sup> Corresponding author (Tiit.Kutser@sea.ee).

### Acknowledgments

I am grateful to Liis Sipelgas and Andres Jaanus, who provided in situ measurements data, and Niklas Strömbeck and Sara Jonasson, who provided the cyanobacterial culture and its specific absorption and scattering coefficient spectra. I also wish to thank the anonymous reviewer and Arnold Dekker, whose comments and suggestions helped to improve the manuscript substantially.

The autonomous flow-through systems on ships-of-opportunity only map chlorophyll content along their routes. Moreover, they take water from a fixed depth. It is assumed that the top water layer is well mixed and that the concentration of chlorophyll is constant in the upper mixed layer. This assumption is true in the case of "normal conditions," when algae that cannot control their vertical movement dominate the waters. Cyanobacteria, however, can regulate their buoyancy and in calm weather tend to keep themselves close to the water surface, quite often forming very dense accumulations just below the water surface and surface scums.

Accumulation of aggregations of cyanobacterial cells just below the water surface and surface scums are so distinct that the extent of the blooms can be mapped using almost any remote sensing instrument. For example, broadband sensors like AVHRR (Kahru et al. 1993; Håkanson and Moberg 1994), multispectral sensors such as CZCS (Siegel et al. 1999) and SeaWiFS (Joint and Groom 2000; Siegel and Gerth 2000), and synthetic aperture radars (Svejkovsky and Shandley 2001) have been used to map the extent of cyanobacterial blooms.

A single broad band of AVHRR (often used for mapping the extent of algal blooms) in the visible part of the spectrum does not allow discrimination between a bloom of cyanobacteria, a bloom of other algae species, increased turbidity due to suspended particulate inorganic matter, and surface pollution. The detection of cyanobacteria using AVHRR has been mainly done based on logical deduction. An increased water-leaving signal in the middle of the Baltic Sea cannot be caused by resuspension of sediments or increased river inflow, as most of the particles sink before reaching the middle of the sea. It is known that cyanobacteria are the dominating species in the Baltic Sea during summer months. Thus, the main cause for increased radiance detected by the AVHRR was probably a cyanobacterial bloom. The amount of in situ data to verify the presence of cyanobacteria is often lacking, or the number of in situ sampling stations is inadequate to develop algorithms for quantitative mapping of cyanobacteria in the bloom. The same logic has been used in interpreting radar data. The radar beam cannot penetrate water deeper than a few millimeters, giving only information about surface roughness. Increased roughness in summer months is attributed to cyanobacterial blooms.

This study clarifies why the current remote sensing methods have failed in quantitative monitoring of chlorophyll during cyanobacterial blooms, especially in the cases in which extensive subsurface accumulations and surface scums occur; it is also the study's goal to roughly assess the extent of chlorophyll concentrations in the bloom. High spectral and spatial resolution satellite data provide new opportunities in studying cyanobacterial blooms, and a novel approach for water bodies is proposed to make better use of the hyperspectral information available.

## Methods

*Remote sensing instruments*—Hyperion and Advanced Land Imager (ALI) images of the northwestern part of the Gulf of Finland were acquired on 14 July 2002. Hyperion is

the first civilian hyperspectral imager in space (Pearlman et al. 2003). Both the Hyperion and ALI instruments are part of NASA's New Millennium Program (NMP) and are on-board EO-1 satellite (<http://eo1.gsfc.nasa.org>), which was launched on 21 November 2000. NMP is an initiative to demonstrate advanced technologies for future space missions. New data acquisition requests of EO-1 data can be made through the U.S. Geological Survey web page (<http://eo1.usgs.gov>).

Hyperion is a pushbroom-type imaging spectrometer that provides radiometrically calibrated data. It is capable of resolving 196 spectral bands in the 400–2,500-nm region with a 30-m spatial resolution. Each spectral band is 10 nm wide, and band spacing is about 11 nm. Thus, Hyperion provides spectrally continuous data for the visible and short-wave infrared part of the spectrum instead of the discrete (and sometimes broad) bands of current imagers (Landsat ETM, SPOT, IKONOS, SeaWiFS, MODIS, and MERIS). The instrument can image a  $7.65 \times 185$ -km area, has 16-bit radiometric resolution, and its signal-to-noise ratio is between 140 and 192 (in wavelength range, 550 and 700 nm), according to the on-orbit calibration.

ALI is a prototype of the next-generation Landsat sensor with improved spectral and radiometric resolution and substantial mass, volume, and cost savings. Its spectral bands in the visible part of the spectrum are practically identical to other multispectral sensors like Landsat and IKONOS. ALI has 10 bands: a panchromatic (480–690 nm) with 10-m spatial resolution and nine spectral bands (*see* <http://eo1.usgs.gov/instru/ali.asp>) with 30-m spatial resolution. Its signal-to-noise ratio is 250:1. The ALI footprint is  $37 \times 185$  km. ALI and Hyperion footprints overlap, and a Hyperion image covers approximately one fourth of the ALI footprint. EO-1 is in the same orbit with Landsat 7 ETM, imaging the same area 1 min later. The EO-1 sensors are pointable, thus allowing shorter revisiting times than are allowed by the Landsat 16-d cycle.

*Atmospheric correction*—Atmospheric correction of the Hyperion image was performed using the Fast Line-of-Sight Atmospheric Analysis of Spectral Hypercubes (FLAASH) software package in ENVI (by Research Systems). The FLAASH module was developed by Spectral Sciences under the sponsorship of the U.S. Air Force Research Laboratory (Adler-Golden et al. 1999). FLAASH is designed for atmospheric correction of hyperspectral data. It incorporates MODTRAN 4 radiation transfer code with all MODTRAN atmosphere and aerosol types to calculate a unique solution for each image. FLAASH also includes a correction for the "adjacency effect," provides an option to compute a scene-average visibility (aerosol/haze amount), and utilizes the most advanced techniques for handling particularly stressing atmospheric conditions (such as clouds). FLAASH output is scaled radiance reflectance that equals to irradiance reflectance in the case of Lambertian surfaces. A mid-latitude summer atmosphere parameter (water vapor  $2.92 \text{ g cm}^{-2}$ ) and marine aerosols together with automatic aerosol retrieval were used in FLAASH to correct the Hyperion image.

As ALI is a multispectral sensor, we could not use this version of FLAASH for atmospheric correction. Therefore,

the empirical line method (Moran et al. 2001 and references within the article) was used to derive an atmospheric correction of the ALI image. The empirical line method requires knowledge about reflectance of at least one target within an image (Moran et al. 2001). This target reflectance may be measured during image acquisition or estimated from historical data. We made use of the atmospherically corrected Hyperion image. We assumed that the reflectance spectra obtained from the Hyperion image are real reflectances of different objects. Targets with different reflectance (lakes, sea, a turbid bay, cyanobacterial bloom at sea, fields, road, forest) were selected to cover the whole range in reflectance values available in the image (excluding clouds). Average radiance spectra for each target were compared to corresponding average reflectance spectra from the atmospherically corrected Hyperion image. Hyperion continuous spectral data was recalculated to simulate discrete ALI bands, and empirical algorithms were derived for each ALI band that enable us to predict apparent pixel reflectance spectra from the top of the atmosphere radiance values.

*Bio-optical modeling*—Gordon et al. (1975), in their Monte Carlo study, were able to fit the irradiance reflectance just beneath the water surface with a polynomial function of absorption and backscattering coefficients. By ignoring all terms other than the dominant first one, the polynomial equation can be simplified to

$$R(0^-, \lambda) = C \frac{b_b(\lambda)}{a(\lambda) + b_b(\lambda)} \quad (1)$$

where  $b_b(\lambda)$  is the total backscattering coefficient,  $a(\lambda)$  is the total absorption coefficient, and where the value of  $C$  depends on the solar zenith angle (for sun at the zenith,  $C = 0.32$ ; Gordon et al. 1975). It is obvious that an expression such as that seen in Eq. 1 contains assumptions regarding the light field and the average shape of the volume-scattering function.

Further Monte-Carlo studies (Kirk 1984) have found the coefficient  $C$  to be a function of solar altitude that is reasonably well expressed as a linear function of  $\mu_0$ , the cosine of the zenith angle of the refracted photons:

$$C(\mu_0) = -0.629\mu_0 + 0.975 \quad (2)$$

For sun at zenith, this relationship predicts  $C = 0.346$  (Kirk 1984) and  $C = 0.440$  in our case, in which  $\mu_0 = 0.85$  (the solar zenith angle during the EO-1 overpass was  $42.6^\circ$ ). From Eqs. 1 and 2, it follows that the irradiance reflectance just below the water surface can be calculated by

$$R(0^-, \lambda) = (-0.629\mu_0 + 0.975) \frac{b_b(\lambda)}{a(\lambda) + b_b(\lambda)} \quad (3)$$

As the light passes through the water–air interface, it undergoes refraction that increases its angle to the vertical. Combining these effects with the effect of internal reflection, Austin (1980) proposed the factor of 0.544 for relating radiance just above the surface with radiance just below the surface. Thus, we can calculate the diffuse component of remote sensing reflectance just above the water surface thus:

$$r_D(\lambda) = 0.544(-0.629\mu_0 + 0.975) \frac{b_b(\lambda)}{a(\lambda) + b_b(\lambda)} \quad (4)$$

The total absorption and backscattering coefficients are additive over the constituents of the medium by the definition of inherent optical properties (which requires the absence of multiple interactions). We assume that there are three optically active components in the water: phytoplankton, colored dissolved organic matter (CDOM), and suspended matter. Under these conditions, the total spectral absorption coefficient,  $a(\lambda)$ , is described by

$$a(\lambda) = a_w(\lambda) + a_{ph}^*(\lambda)C_{chl} + a_{CDOM}(\lambda) + a_{SM}^*(\lambda)C_{SM} \quad (5)$$

where  $a_w$  is the absorption coefficient of pure water,  $a_{ph}^*(\lambda)$  is the chlorophyll-specific spectral absorption coefficient of phytoplankton,  $a_{CDOM}(\lambda)$  is the spectral absorption coefficient of CDOM, and  $a_{SM}^*(\lambda)$  is the specific absorption coefficient of suspended matter.  $C_{chl}$  and  $C_{SM}$  are concentrations of chlorophyll  $a$  and total suspended matter.

The total spectral backscattering coefficient  $b_b(\lambda)$  can be described thus:

$$b_b(\lambda) = 0.5b_w(\lambda) + b_{b,ph}^*(\lambda)C_{chl} + b_{b,SM}^*(\lambda)C_{SM} \quad (6)$$

where  $b_w$  is the scattering coefficient of pure water and where it is assumed that the backscattering probability is 50% in pure water.  $b_{b,ph}^*$  is chlorophyll-specific backscattering coefficient of phytoplankton and  $b_{b,SM}^*$  is the suspended sediment-specific spectral backscattering coefficient of suspended matter.

*Model parameters*—Models, similar to that described above, are proposed by a number of authors (*see* list of models in Dekker et al. 2001a). The main differences between the models lie in the number of optically active components and the specific absorption and backscattering coefficients used. In the present study we assume that there are three optically active substances in the water: phytoplankton, suspended matter, and CDOM. The amount of CDOM, as well as absorption and backscattering due to suspended matter, are often expressed through empirical functions of  $C_{chl}$ . This is acceptable in the case of oceanic waters but not in the case of coastal and inland waters, where concentrations of optically active substances are not correlated with chlorophyll  $a$  concentration.

In our model the values of absorption and scattering coefficients of pure water were taken from Smith and Baker (1981). The absorption by CDOM is expressed as a function of the absorption coefficient of filtered water sample at wavelength 400 nm,  $a_{CDOM}(400)$ , and slope factor,  $S$ , by following formula:

$$a_{CDOM}(\lambda) = a_{CDOM}(400)\exp[-S(\lambda - 400)] \quad (7)$$

According to estimations by Mäekivi and Arst (1996),  $S = 0.017$  gives the best result in the case of the Baltic Sea and the Estonian and Finnish lakes. The specific absorption coefficient of suspended matter was taken from Kutser (1997), and specific scattering coefficients of suspended matter, as well as backscattering probabilities (backscattering to scattering ratio), were taken from a study by Kutser et al. (2001).

The bloom in the Gulf of Finland was dominated by non-

toxic *Aphanizomenon flos-aquae* in the first half of July, when the subsurface accumulations of algae started to build up (Alg@line monitoring results, [www.helcom.fi/environment/algalblooms.html](http://www.helcom.fi/environment/algalblooms.html)), but the fraction of toxic *Nodularia spumigena* increased in the phytoplankton flora and grew more abundant in the open-water areas, where they dominated during the second half of July. Chlorophyll-specific absorption and scattering coefficients of *A. flos-aquae* cultures (Strömbeck and Jonasson pers. comm.) were used in the model. It would have been desirable to use a model similar to that of Dekker et al. (2001a), in which phycocyanin is included as a separate component. Unfortunately, there is not enough data available about bio-optical properties and the concentration range of phycocyanin in the Baltic Sea cyanobacteria species. Phycocyanin absorption is included in the *A. flos-aquae*-specific absorption coefficient spectrum used in the modeling, but its concentration is unknown. Therefore, the amount of phycocyanin is covarying with changes in chlorophyll.

The backscattering probability of phytoplankton is highly variable (Stramski et al. 2001). The backscattering probability of cyanobacteria varies between 0.5% (Ahn et al. 1992) and 1.7% (Dekker 1993). A backscattering probability of 1.5% was used in the present study. It is often assumed that the backscattering probability is constant over the visible part of spectrum. However, the results by Ahn et al. (1992) indicate that the cyanobacteria have backscattering probability spectra that differ from that of other algae. Therefore, a mean backscattering probability spectrum of cyanobacteria, normalized to 560 nm, as calculated from data published by Ahn et al. (1992), was used. The absorption and backscattering coefficients of the optically active substances, used in the model, are shown in Fig. 1.

Concentrations of nonchlorophyllous suspended matter and  $a_{CDOM}(400)$  were fixed in the model simulations and were chosen to be similar to the values observed during field measurements in the southwestern part of the Gulf of Finland (Sipelgas pers. comm.), carried out at the same time with the Hyperion and ALI image acquisition. It was assumed that the concentration of suspended matter is the sum of nonchlorophyllous and organic particles and the relationship by Gons et al. (1992), where 1 mg m<sup>-3</sup> chlorophyll is approximately equal to 0.07 mg L<sup>-1</sup> of suspended matter, was used to estimate the  $C_{SM}$ . The nonchlorophyllous suspended matter concentration was taken to be 2 mg L<sup>-1</sup>, and  $a_{CDOM}(400) = 0.71$  m<sup>-1</sup>.

The aim of this study was not to give chlorophyll estimations that were as accurate as possible but rather to study the potential extent of variability in chlorophyll values during cyanobacterial blooms. Therefore, a large range of chlorophyll concentrations was chosen for the model simulations. Concentrations of chlorophyll used in the model simulations were 1, 2, 4, 8, 16, 32, 64, 128, 256, 512, and 1,024 mg m<sup>-3</sup>. Some of the Hyperion spectra from the most dense bloom areas were similar to reflectance spectra of terrestrial vegetation. Therefore, a model run was made where absorption and scattering due to water molecules was turned off. The modeled spectra were collected into a spectral library that was used for mapping chlorophyll concentration in the Gulf of Finland from the Hyperion image. Some of

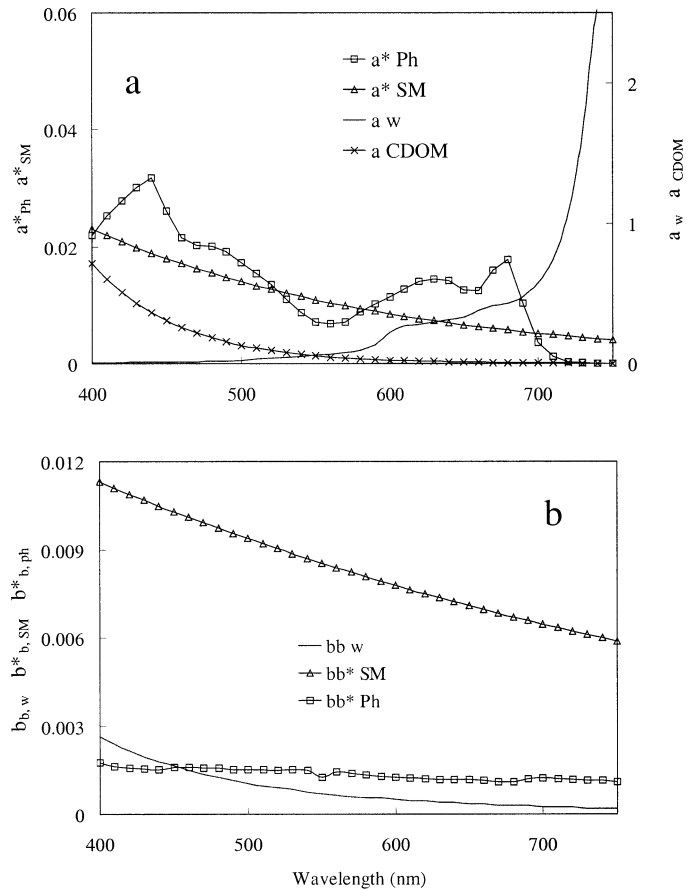


Fig. 1. Spectra of absorption (a) and backscattering coefficients (b) used in the model.  $a_w$  is the absorption coefficient of pure water (m<sup>-1</sup>; Smith and Baker 1981);  $a_{CDOM}$  is the absorption coefficient of colored dissolved organic matter (m<sup>-1</sup>; Eq. 7);  $a_{SM}^*$  is the specific absorption coefficient of suspended matter (m<sup>2</sup> mg<sup>-1</sup>; Kutser 1997);  $a_{Ph}^*$  is the chlorophyll-specific absorption coefficient of cyanobacterium *Anabaena flos-aquae* (m<sup>2</sup> μg<sup>-1</sup>; Strömbeck and Jonasson pers. comm.);  $b_w$  is the backscattering by pure water (m<sup>-1</sup>, calculated from Smith and Baker [1981]);  $b_{SM}^*$  is the specific backscattering coefficient of suspended matter (m<sup>2</sup> mg<sup>-1</sup>; Kutser et al. 2001); and  $b_{Ph}^*$  is the chlorophyll-specific backscattering coefficient of cyanobacterium *A. flos-aquae* (m<sup>2</sup> μg<sup>-1</sup>) calculated from scattering spectra provided by Strömbeck and Jonasson (pers. comm.), mean normalized backscattering probability spectra from Ahn et al. (1992), and a 1.5% backscattering probability.

the modeled spectra used in image classification are shown in Fig. 2.

**Image classification**—Modern image processing software packages (such as Research Systems ENVI) include several procedures to produce classification maps given a spectral library of end-members—or “pure” examples are available. It is also possible in some packages to derive end-members for a spectral library directly from the image. However, the number, relevance, and “quality” of such end-members is variable and image specific. For example, the quality of image-derived end-members depends on the illumination condition during image acquisition and atmospheric correction of the image. Therefore, it is preferable to use measured (in

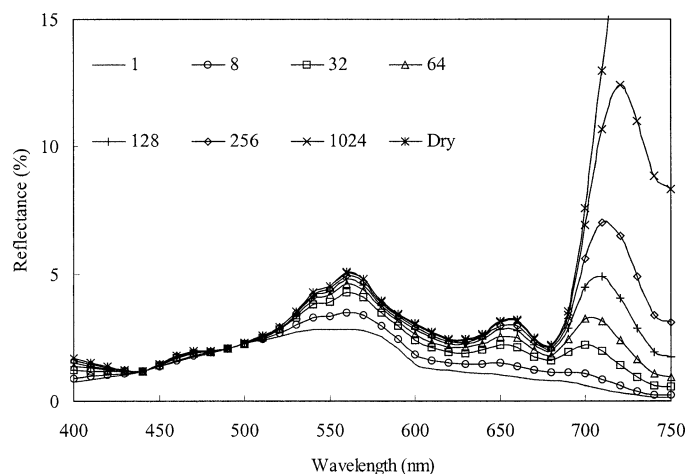


Fig. 2. Part of the spectra from the modeled reflectance spectral library used in mapping chlorophyll in the Hyperion image. Concentrations of chlorophyll in the legend are in  $\text{mg m}^{-3}$ . “Dry” indicates that the spectra were modeled by turning off the absorption and scattering of water molecules.

situ or in laboratory) end-member spectra or modeled spectral libraries. The latter was used in this study, as there is not enough data available on optical properties of cyanobacterial blooms.

In this article we have used the Spectral Angle Mapper (SAM) with the modeled spectral library to produce a chlorophyll concentration map from the Hyperion image. SAM (Kruse et al. 1993) is a spectral classification that uses an  $n$ -dimensional angle to match pixels to reference spectra. The algorithm determines the spectral similarity between two spectra by calculating the angle between the spectra, treating them as vectors in a space with dimensionality equal to the number of bands. This technique, when used on calibrated reflectance data, is relatively insensitive to illumination and albedo effects, since it is invariant to multiplication of signatures by a constant. In operation, SAM compares the angle between the end-member spectrum vector and each pixel vector in  $n$ -dimensional space and selects the end-members with minimum angle. Smaller angles represent closer matches to the reference spectrum. Pixels further away than a specified maximum angle threshold in radians are not classified. The suitability of different maximum angles was tested in the chlorophyll classification process.

## Discussion

*Image data and processing*—Neither Hyperion nor ALI was designed for a water environment. However, Brando and Dekker (2003) have shown that Hyperion can be used to map optical water quality (concentrations of chlorophyll, CDOM, and suspended matter) in complex estuarine and coastal systems. It has also been shown (Kutser et al. 2002) that Hyperion can be used to map shallow-water benthic habitat. Intensity of the signal in the bloom areas was more similar to that of shallow-water habitats or even terrestrial vegetation than to coastal waters. Thus, the Hyperion data quality was higher and atmospheric correction of the image

easier than it would have been in the case of clear oceanic waters or CDOM-rich lakes, in which the water-leaving radiance is low. Hyperion water reflectance spectra obtained after atmospheric correction by FLAASH were similar to those observed by different authors (Arst et al. 1996; Kutser et al. 1997, 1998, 2001; Kallio et al. 2001) in the same study area (the Gulf of Finland, Finnish and Estonian lakes) or by other authors in optically similar water bodies (Dekker et al. 2001a,b; Pierson and Strömbeck 2001). It allows us to assume that the atmospheric correction was successful. It must be noted that FLAASH is designed for land surfaces. Therefore, the obtained water reflectance values may also contain a certain amount of Fresnel reflectance. Nevertheless, the water reflectance spectra obtained from the Hyperion image using FLAASH were realistic in shape and magnitude.

Atmospheric correction of the ALI image was performed using atmospherically corrected Hyperion data and the empirical line method. The first four ALI bands (450–515 nm, 525–605 nm, 630–690 nm, and 775–805 nm) were corrected. It is generally assumed that water-leaving radiance is zero in the near-infrared part of spectrum because of strong absorption by water molecules. This makes the use of ALI band 4 questionable in water remote sensing, as the reflectance values in this band must be zero in case of water pixels (excluding the Fresnel skylight reflectance). However, the band 4 reflectance values contain useful information about the surface scum, as will be shown later.

Different angles were used while classifying the Hyperion image with SAM and the modeled spectral library. The angle of 0.5 rad proved to be optimal, as some of the image areas remained unclassified in the case of smaller angles, and the classification results became noisy when larger angles were used.

*Spectral signatures of the cyanobacterial bloom*—Some reflectance spectra collected from the bloom area in the Hyperion image are shown in Fig. 3. The spectra are similar to those measured in cyanobacteria cultures (Quibell 1992; Richardson 1996) and in natural blooms from aboard a boat (Jupp et al. 1994; Kutser et al. 1997; Schalles et al. 1998) or using airborne spectrometers (Dekker et al. 1992; Jupp et al. 1994).

Cyanobacterial blooms can be divided into three states from the optical and remote sensing point of view. First of all there is a state in which single cells or aggregations of the cells are distributed relatively uniformly within the top mixed layer of the water body. This state is the easiest to handle from the remote sensing and water-sampling point of view, as the flow-through systems on ships-of-opportunity and water sampling from research vessels give adequate chlorophyll concentrations. In calm weather conditions, the aggregations of cyanobacteria floating near the water surface form a dense souplike mixture. The subsurface blooms are optically similar to those of submerged vegetation (Dekker et al. 2001a), tidal mats (Paterson et al. 1998), or even different coral reef benthic habitats (Kutser et al. 2003). Typical features in the reflectance spectra of waters dominated by cyanobacteria are an absorption feature near 630 nm, caused by phycocyanin (Dekker et al. 1992; Richardson 1996), a peak near 650 nm, and high reflectance values near 700 nm.

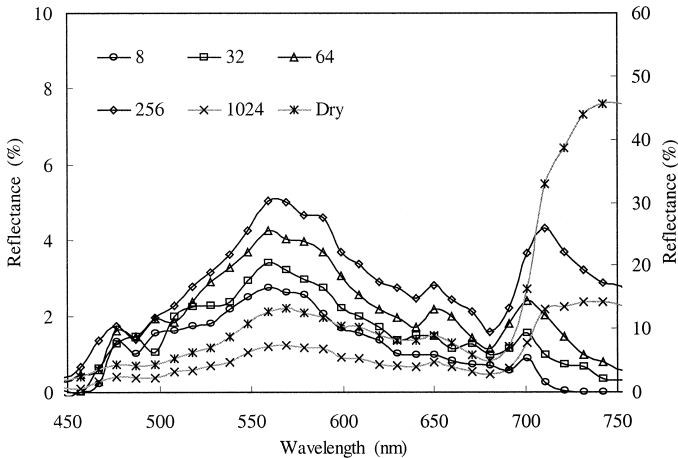


Fig. 3. Reflectance spectra of some pixels taken from the atmospherically corrected Hyperion image. The numbers in the legend indicate concentrations of chlorophyll ( $\text{mg m}^{-3}$ ), as were classified by Spectral Angle Mapper and the modeled spectral library. Reflectance values for the classes “1,024” and “Dry” are given in the right axis. “Dry” means that the Hyperion reflectance spectrum is similar to the spectral library spectrum, which was modeled without the absorption and backscattering by water molecules.

The later feature is also common in reflectance spectra of other algae if they are present in very high quantities ( $>60 \text{ mg m}^{-3}$ ; Quibell 1992). The peak near 700 nm, its height, and its width are caused by the combined effect of high backscattering and fluorescence from the algae in the red and near-infrared part of the spectrum and exponentially increasing absorption of light by water itself in the same spectral region. Location and width of the peak are often used (Gitelson 1992; Dekker 1993; Jupp et al. 1994; Kallio et al. 2001, 2003) to estimate chlorophyll concentration in water.

Measured reflectance data (Quibell 1992; Kutser et al. 1997) and the Hyperion spectra (Fig. 3) show that there is no peak near 650 nm in the reflectance spectra of cyanobacteria in the case in which concentration of chlorophyll is less than  $10 \text{ mg m}^{-3}$  (reported maximum in the middle of the Gulf of Finland during the 2002 bloom). The same measurements have also shown that the peak becomes clearly seen when the concentration of chlorophyll is between  $30 \text{ mg m}^{-3}$  and  $50 \text{ mg m}^{-3}$ . Hyperion spectra are in agreement with those results. Laboratory and in situ measurements (Quibell 1992) with waters in which concentration of chlorophyll is higher than  $100 \text{ mg m}^{-3}$  showed that in such cases, the reflectance spectra were still typical for subsurface blooms (peaks near 650 nm and 700 nm) but not for surface scums (high reflectance also beyond 730 nm). Schalles et al. (1998) have found that reflectance spectra of an *Anabaena* bloom, in which chlorophyll concentrations were between 120 and  $280 \text{ mg m}^{-3}$ , were still typical to the subsurface bloom and were similar to the Hyperion spectra that were classified as waters in which the  $C_{Chl}$  values were up to  $256 \text{ mg m}^{-3}$ . Thus, the shapes of Hyperion spectra are in agreement with spectra measured by other authors, and the estimations of  $C_{Chl}$  are in the same concentration range with laboratory data for concentrations up to  $256 \text{ mg m}^{-3}$ .

Reflectance values remain high in the infrared part of the

spectrum when the surface scums occur since the algae cover the water surface and absorption by water molecules does not play a significant role in the spectra detected by a remote sensing instrument. Reflectance spectra of such scums have been measured in the laboratory (Quibell 1992; Richardson 1996) and in the case of natural blooms (Quibell 1992; Jupp et al. 1994). Similar reflectance spectra have been retrieved from the Hyperion image (Fig. 3). This indicates that the surface scum areas with high reflectance values in the infrared part of the spectrum can be separated from the subsurface bloom areas, in which reflectance values decrease with increasing wavelength beyond 700–710 nm.

The scum is optically opaque. This means that remote sensing sensors cannot get any information about water properties below the scum. It is also quite difficult to estimate chlorophyll content in the scum. Optical properties of the scum are more similar to those of terrestrial vegetation than that of water bodies. Vegetation indices, such as the NDVI used in terrestrial remote sensing, or methods similar to the spectral library approach, proposed in the current article for estimating chlorophyll concentration in the water, can be used in an attempt to estimate chlorophyll, phycocyanin, or particulate organic carbon concentrations in the scum. However, more detailed knowledge about the bio-optical properties of surface scums is needed.

Chlorophyll values measured in surface scums for which reflectance spectra have been published vary between  $350 \text{ mg m}^{-3}$  (Jupp et al. 1994) and  $894 \text{ mg m}^{-3}$  (Quibell 1992). Galat and Verdin (1989) have studied surface scums of *Nodularia* in Pyramid Lake, Nevada, where they measured chlorophyll concentrations of up to  $9,790 \text{ mg m}^{-3}$  (average  $468 \text{ mg m}^{-3}$ ) and cell densities of up to  $3.5 \times 10^6 \text{ cells ml}^{-1}$ . Thus, the chlorophyll values in surface scums may be an order of magnitude higher than the highest concentration used in the present study. Unfortunately, Galat and Verdin (1989) did not publish their reflectance data.

Optical properties of the scums may vary depending on age of the scum as a result of photo-oxidation, heat, and the rate of healthy versus decaying cells in the scum (Sellner 1997). Thus, the amount of chlorophyll in the surface scums may vary dramatically depending on the age of the bloom. Detailed analyses of optical properties of the surface scums have to be carried out simultaneously with studies on the development of the bloom before conclusions can be made about the limits of remote sensing in quantitative mapping of chlorophyll (phycocyanin, particulate organic carbon) concentrations in surface scums. However, a similarity in the reflectance spectra of surface scums detected by Hyperion and in those measured by Jupp et al. (1994) and Quibell (1992) indicate that concentration of chlorophyll in the Gulf of Finland (in the areas where the surface scums occurred) was at least approximately  $300 \text{ mg m}^{-3}$ , rather than maximally  $6\text{--}8 \text{ mg m}^{-3}$ , as was reported by autonomous measuring systems on the ships-of-opportunity (Jaanus pers. comm.) at the time of Hyperion image acquisition.

Our modeling results indicate that the area covered with surface scums was relatively small compared to the areas in which the cyanobacteria were below the water surface at the time of the image acquisition. We also estimated surface scum areas in the ALI image using band 4 (775–805 nm).



Fig. 4. A part ( $37.6 \times 57.2$  km) of a true color image of Advanced Land Imager (ALI) acquired on 14 July 2002 in the northwestern part of the Gulf of Finland. Areas in which presence of surface scums was estimated using band 4 (775–805 nm) reflectance values are shown in red. The Hyperion footprint seen in Fig. 5 is indicated with the frame.

Potential surface scum areas (in which the band 4 reflectance was higher than 5%) are indicated in red in Fig. 4. Visual observations of the Hyperion and ALI images indicate that the surface scum areas are actually larger. One of the reasons for this is that the chlorophyll classes of 512 and  $1,024 \text{ mg m}^{-3}$  were used as separate classes during the classification process. Reflectance spectra of those two classes, however, are similar to reflectance spectrum of the “DRY” class we defined as surface scum. Data available with regard to surface scums (Galat and Verdin 1989; Quibell 1992; Jupp et al. 1994) also indicate that such high chlorophyll values occur only in surface scums. Thus, the actual area of surface scums can be described by the sum of three classes: “512,” “1,024,” and “Dry.” Another reason why part of surface scum areas is not identified in the ALI and Hyperion images is because of the spatial resolution of the satellites. For example, the comblike structures that occur in both images are most likely stripes of surface scum blown away from the area in which the algae first surfaced. The width of those structures is less than 30 m, and the resulting reflectance spectra are mixtures of relatively clear water reflectance and scum reflectance (i.e., they are similar to dense subsurface bloom spectra).

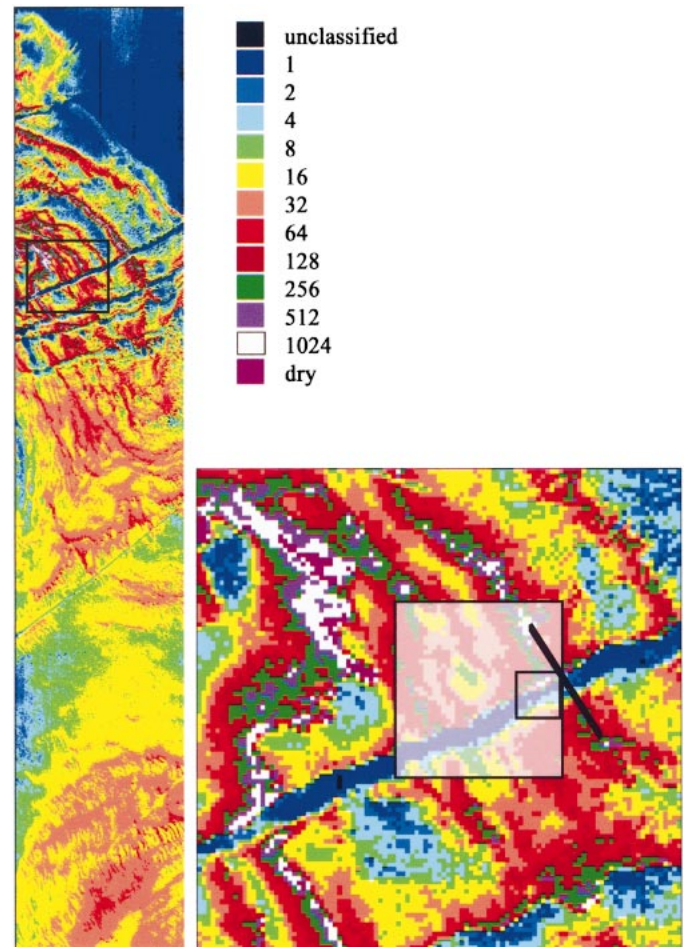


Fig. 5. Chlorophyll map of the northwestern part of the Gulf of Finland and the zoom-in area with the ship track under investigation. Modeled spectral library and Spectral Angle Mapper with a maximum angle of 0.5 rad were used to classify the image. Numbers in the legend indicate chlorophyll *a* concentrations in  $\text{mg m}^{-3}$  corresponding to each class. The transect across a ship track (thick black line) and areas equal to  $1 \times 1$  km and  $240 \times 270$  m hypothetical satellite pixels, used in the analysis, are indicated in the zoom image. Size of the area shown in the Hyperion image is  $7 \times 42.3$  km.

*Depth of penetration*—The main limiting factor for remote sensing estimates of chlorophyll concentration of a water body is the depth of penetration at which the signal that can be detected by a remote sensing sensor is originated. The depth of penetration is inversely proportional to the diffuse attenuation coefficient. The vertical attenuation coefficient for downward irradiance at the midpoint of the euphotic zone,  $K_d(z_{10\%})$  (the depth at which the downwelling irradiance has decreased to 10% of its subsurface value) can be calculated using the following formula by Kirk (1984):

$$K_d(z_{10\%}) = \frac{1}{\mu_0} [a^2 + (0.473\mu_0 - 0.218ab)]^{1/2} \quad (8)$$

where  $a$  is the total absorption coefficient and  $b$  is the total scattering coefficient. Our model enables us to calculate  $K_d(z_{10\%})$  according to Eq. 8. Maximum depth of penetration

(at wavelength around 580 nm) was 2.44 m when  $C_{chl} = 1 \text{ mg m}^{-3}$  and was just 12 cm when  $C_{chl} = 512 \text{ mg m}^{-3}$ . Thus, the layer in which most of the remote sensing signal is derived is very thin in the case of a dense subsurface bloom, and it is practically zero in the case of surface scums.

*Spatial signatures of the cyanobacterial bloom*—Cyanobacterial blooms are extremely patchy. This is seen in the ALI image of the western part of Gulf of Finland (Fig. 4). Cyclonic eddies, mushroom-shaped jets, and ship tracks are the physical features clearly seen in the image. Northerly winds have blown the surface scum away from the locations at which the scum surfaced. This created the comblike structures near the places in which the surface scums occurred. One can also observe that the bloom occurs in the middle of the Gulf of Finland and that coastal areas are free of the bloom.

Clear differences between ship tracks and surrounding areas indicate that the amount of cyanobacteria in the ship track area is different from the surrounding bloom areas. This is an indicator that the flow-through systems on ships-of-opportunity cannot provide reliable estimations of phytoplankton in the water during cyanobacterial blooms. The ships take water from a depth of ca. 5 m (Leppänen et al. 1995; Rantajärvi et al. 1998). The sample from this depth is not correlated with the amount of cyanobacteria in the surface layer detected by remote sensing sensors, especially in the case of surface scums.

The same problem occurs when taking water samples from research vessels. The vessel disturbs the water surface, pushing the scum and subsurface aggregations away from the ship. We have made attempts to drift into dense bloom area to collect water samples from the locations in which the surface scum occurred to get more representative estimations of chlorophyll content than conventional (integrated) water samples provide. It was practically impossible to collect water samples containing the subsurface aggregations or surface scums from aboard a research vessel. Surface scum and the subsurface aggregations tend to move away from any water-sampling device. Even if some aggregations or parts of scum are captured, they tend to stay in the sampler, thereby reducing the concentration of chlorophyll measured in the laboratory. Surface scum samples can be collected from a small boat (Galat and Verdin 1989). However, lowering a boat from a larger research vessel during regular monitoring cruises is often not possible as a result of tight schedules. The standard procedure in monitoring the state of the Baltic Sea (HELCOM, [www.helcom.fi](http://www.helcom.fi)) is taking integrated water samples. The concentration of chlorophyll is even more diluted in the process. Thus, the amount of cyanobacteria detected by a remote sensing sensor and the concentration of chlorophyll measured from water samples using standard sampling techniques are not comparable with each other.

*Variability in chlorophyll values within the bloom*—The chlorophyll map obtained from the Hyperion image using the modeled spectral library and the SAM algorithm is shown in Fig. 5. A few pixels were collected along a randomly chosen transect perpendicular to a ship track to assess

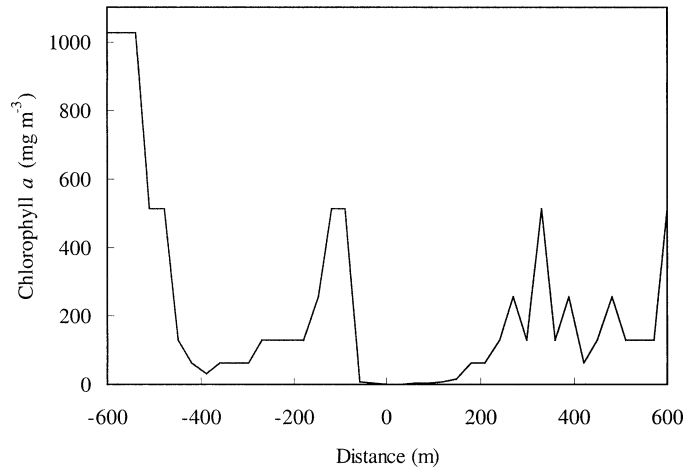


Fig. 6. Chlorophyll concentrations along a randomly chosen transect across a ship track shown in Fig. 5. Distances are given from the middle of the ship track.

the differences in chlorophyll concentrations between the ship track area and the surrounding bloom. The variation in chlorophyll along this transect is shown in Fig. 6. Chlorophyll concentrations in the ship track area were estimated to be up to  $8 \text{ mg m}^{-3}$ , a value that was typical for the open parts of the Gulf of Finland at the time of image acquisition, according to monitoring measurements (Jaanus pers. comm.). Chlorophyll concentrations in the middle of the Gulf of Finland measured from ferries traveling between Tallinn and Helsinki (a few miles east from the ALI image in Fig. 4) were  $6\text{--}8 \text{ mg m}^{-3}$ , close to the peak chlorophyll values (around  $10\text{--}12 \text{ mg m}^{-3}$ ) found in the open Baltic Sea during cyanobacterial blooms (Rantajärvi et al. 1998; Alg@line web page). These values are significantly lower than the chlorophyll values obtained just outside the ship track (up to  $1,024 \text{ mg m}^{-3}$  along the randomly chosen transect shown in Fig. 5). Thus, the chlorophyll values obtained from the ship track area in the Hyperion image are similar to monitoring data from the ships-of-opportunity. However, those chlorophyll concentrations are up to two orders of magnitude lower than estimated from Hyperion data just tens of meters away from the ship track.

Most of the satellite sensors do not have a spatial resolution that is comparable with the 30-m resolution of Hyperion. Marine remote sensing satellites (SeaWiFS, MERIS reduced resolution) have spatial resolutions of approximately 1 km. Freely available MODIS Terra and Aqua data also have 1-km spatial resolution for most of the bands. Two MODIS bands have 250-m spatial resolution. MERIS full-resolution data will provide information with nearly similar ( $290 \times 260 \text{ m}$ ) spatial resolution. Randomly chosen areas were selected in the Hyperion chlorophyll map (Fig. 5) to study the variability in chlorophyll concentrations that occurs within a hypothetical  $1 \times 1\text{-km}$  pixel and a  $240 \times 270\text{-m}$  pixel. The areas were selected to mimic a real water-sampling situation (i.e., they contain large amounts of pixels from a ship track that would have occurred while sampling from a research vessel). The results are shown in Figs. 7 and 8. Within-pixel variability in chlorophyll values is remark-

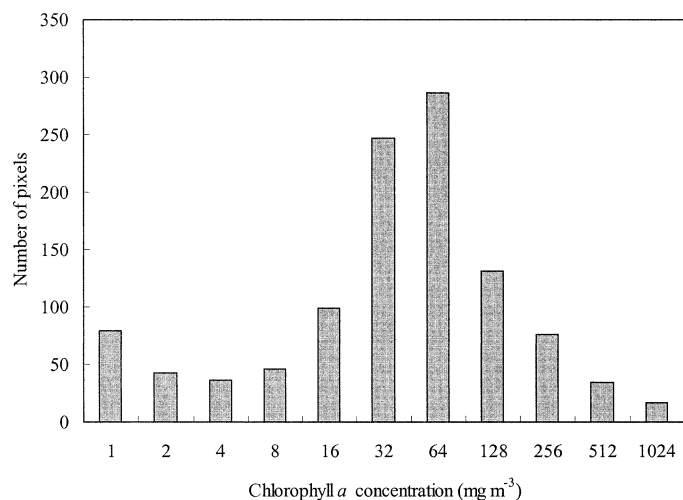


Fig. 7. Concentrations of chlorophyll within a randomly chosen  $1 \times 1$ -km area in the Hyperion image (Fig. 5) that is approximately equivalent to one pixel of MODIS spectral bands or SeaWiFS full resolution or MERIS reduced resolution (acquired routinely).

able in both cases. Taking the hypothetical pixels from the bloom areas that are not disturbed by ships would have given chlorophyll concentrations that differed even more from water-sampling results.

The Hyperion image shows that the patchiness of cyanobacterial blooms and the coarse spatial resolution of most satellite sensors are some of the reasons why quantitative mapping of cyanobacterial blooms has been unsuccessful in the case of satellite remote sensing. This is the main cause of errors in chlorophyll estimation, if we assume that in situ measurements can give us adequate chlorophyll values at least for a small point within a satellite pixel. The real sampling situation in the case of using standard methods, however, indicates that it is practically impossible to collect water samples that would be representative of the natural conditions when subsurface aggregations of cyanobacteria or surface scums occur. Ships and water samplers destroy the natural structure of the bloom area unless specially designed sampling procedures are developed and used (similar to Galat and Verdin [1989], for example). Thus, the amount of chlorophyll detected by a remote sensor will not be the same as that measured from water samples, even if spatial resolution of a remote sensing sensor is equal to the size of the water sampler.

One of the problems related to interpretation of remote sensing data is atmospheric correction. Current standard atmospheric correction procedures, developed mainly for ocean waters, fail in the case of multicomponental waters such as the Baltic Sea (Darecki and Stramski 2004). Atmospheric corrections suitable for turbid waters have been proposed (Hu et al. 2000), but they also fail in the case of the Baltic Sea (Reinart pers. comm.). It is not difficult to understand why the atmospheric correction procedures fail in the case of dense cyanobacterial blooms. It is assumed in the atmospheric models that the water-leaving radiance is zero in the near-infrared part of spectrum. Figure 3 shows that this is not the case during cyanobacterial blooms. Pixels

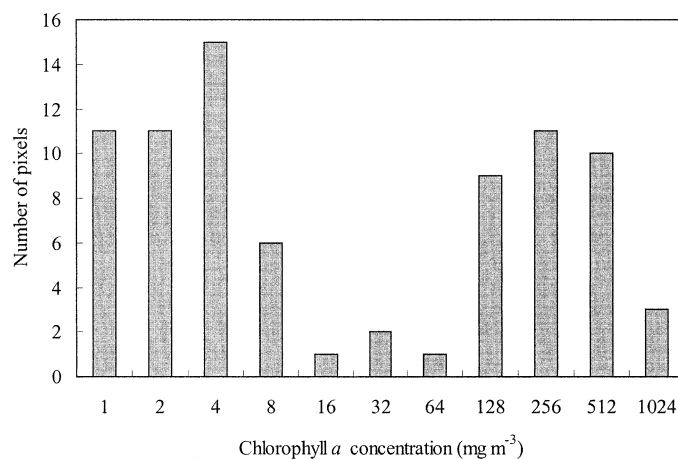


Fig. 8. Concentrations of chlorophyll within a randomly chosen  $240 \times 270$ -m area in the Hyperion image (Fig. 5) that is approximately equivalent to one MODIS high-resolution pixel and MERIS full-resolution pixel.

with high water-leaving radiance are often masked out as measurement and atmospheric correction errors in Level 2 data products. For example, most of the bloom areas seen in the Hyperion and ALI images (Figs. 2, 3) are masked out in MODIS standard algorithm chlorophyll maps acquired 30 min later than the Hyperion and ALI images.

The results presented indicate that the concentration of chlorophyll in cyanobacterial blooms is much higher than has been reported by conventional water-sampling programs, ship-of-opportunity measurements, and previous remote sensing estimates. This is caused by the horizontal and vertical structure of cyanobacterial blooms. Conventional water-sampling programs and ships-of-opportunity cannot provide reliable chlorophyll values, as it is assumed that the phytoplankton is uniformly distributed in the top mixed layer of the water column. This assumption is true in the case of other pelagic algae. Cyanobacteria, however, can regulate their buoyancy and tend to move close to the water surface, often forming surface scums. Research vessels destroy the natural structure of the bloom and cannot provide true chlorophyll values unless special precautions have been taken to collect water samples with the subsurface accumulations and surface scums. The real chlorophyll values in dense cyanobacterial blooms can only be estimated from remote sensing data. This, however, requires detailed knowledge about optical properties of the bloom, knowledge that is currently not available.

The chlorophyll estimation accuracy in cyanobacterial blooms by marine remote sensing satellites is limited as a result of their coarse spatial resolution and the fine spatial phenomena present in a bloom. Results of the current study show that significant changes in chlorophyll concentration occur even at a smaller spatial scale than the 30-m resolution of Hyperion and ALI. Especially when cyanobacterial surface scums occur. Therefore, a single-point in situ measurement is inadequate for validation of satellite chlorophyll estimates during cyanobacterial blooms.

## References

- ADLER-GOLDEN, S. M., AND OTHERS. 1999. Atmospheric correction for short-wave imagery based on MODTRAN 4. *SPIE Proc.* **3753**: 61–69.
- AHN, Y.-H., A. BRICAUD, AND A. MOREL. 1992. Light backscattering efficiency and related properties of some phytoplankters. *Deep-Sea Res.* **39**: 1835–1855.
- ARST, H., S. MÄEKIVI, T. KUTSER, A. REINART, A. BLANCO-SEQUERO, J. VIRTA, AND P. NÖGES. 1996. Optical investigations of Estonian and Finnish lakes. *Lakes Reservoirs Res. Manage.* **2**: 187–198.
- AUSTIN, R. W. 1980. Gulf of Mexico, ocean-colour surface-truth measurements. *Boundary-Layer Meteorol.* **18**: 269–285.
- BRANDO, V. E., AND A. G. DEKKER. 2003. Satellite hyperspectral remote sensing for estimating estuarine and coastal water quality. *IEEE Trans. Geosci. Remote Sensing* **41**: 1378–1387.
- DARECKI, M., AND D. STRAMSKI. 2004. An evaluation of MODIS and SeaWiFS bio-optical algorithms in the Baltic Sea. *Remote Sensing Environ.* **89**: 326–350.
- DEKKER, A. G. 1993. Detection of optical water quality parameters for eutrophic waters by high resolution remote sensing. Ph.D. thesis, Vrije Univ.
- , AND OTHERS. 2001a. Imaging spectrometry of water, p. 307–359. *In* F. D. van der Meer and S. M. de Jong [eds.], *Imaging spectrometry: Basic principles and prospective applications*. Kluwer Academic.
- , T. J. MALTHUS, AND L. M. GODDIJN. 1992. Monitoring cyanobacteria in eutrophic waters using airborne imaging spectroscopy and multispectral remote sensing systems. *Proc. 6th Australasian Remote Sensing Conf.* **1**: 204–214.
- , R. J. VOS, AND S. W. M. PETERS. 2001b. Comparison of remote sensing data, model results and in situ data for total suspended matter (TSM) in the southern Frisian Lakes. *Sci. Total Environ.* **268**: 197–214.
- GALAT, D. L., AND J. P. VERDIN. 1989. Patchiness, collapse and succession of cyanobacterial bloom evaluated by synoptic sampling and remote sensing. *J. Plankton Res.* **11**: 925–948.
- GITELSON, A. A. 1992. The peak near 700 nm on radiance spectra of algae and water: Relationships of its magnitude and position with chlorophyll concentration. *Int. J. Remote Sens.* **13**: 3367–3373.
- GONS, H. J., T. BURGER-WIERSMA, J. H. OTTEN, AND M. RIJKEBOER. 1992. Coupling of phytoplankton and detritus in a shallow, eutrophic lake (Lake Loosdrecht, The Netherlands). *Hydrobiologia* **233**: 51–59.
- GORDON, H. R., O. B. BROWN, AND M. M. JACOBS. 1975. Computed relationships between the inherent and apparent optical properties of a flat, homogeneous ocean. *Appl. Optics* **14**: 417–427.
- HÅKANSON, B. G., AND M. MOBERG. 1994. The algal bloom in the Baltic during July and August 1991, as observed from NOAA weather satellites. *Int. J. Remote Sensing* **15**: 963–965.
- HU, C., K. L. CARDER, AND F. E. MUELLER-KARGER. 2000. Atmospheric correction of SeaWiFS imagery over turbid coastal waters: A practical method. *Remote Sensing Environ.* **74**: 195–206.
- JOINT, I., AND B. GROOM. 2000. Estimation of phytoplankton production from space: Current status and future potential of satellite remote sensing. *J. Exp. Mar. Biol. Ecol.* **250**: 233–255.
- JUPP, D. L. B., J. T. O. KIRK, AND G. P. HARRIS. 1994. Detection, identification and mapping of cyanobacteria—using remote sensing to measure the optical quality of turbid inland waters. *Aust. J. Mar. Freshwat. Res.* **45**: 801–828.
- KAHRU, M. 1997. Using satellites to monitor large-scale environmental change in the Baltic Sea, p. 43–61. *In* M. Kahru and C. W. Brown [eds.], *Monitoring algal blooms: New techniques for detecting large-scale environmental change*. Springer-Verlag.
- , J.-M. LEPPÄNEN, AND O. RUD. 1993. Cyanobacterial blooms cause heating of the sea surface. *Mar. Ecol. Prog. Ser.* **101**: 1–7.
- , ———, ———, AND O. P. SAVCHUK. 2000. Cyanobacteria blooms in the Gulf of Finland triggered by saltwater inflow into the Baltic sea. *Mar. Ecol. Prog. Ser.* **207**: 13–18.
- KALLIO, K., S. KOPONEN, AND J. PULLIAINEN. 2003. Feasibility of airborne imaging spectrometry for lake monitoring—a case study of spatial chlorophyll *a* distribution on two meso-eutrophic lakes. *Int. J. Remote Sensing* **24**: 3771–3790.
- , T. KUTSER, T. HANNONEN, S. KOPONEN, J. PULLIAINEN, J. VEPSÄLÄINEN, AND T. PYHÄLAHTI. 2001. Retrieval of water quality from airborne imaging spectrometry of various lake types in different seasons. *Sci. Total Environ.* **268**: 59–77.
- KIRK, J. T. O. 1984. Dependence of relationships between inherent and apparent optical properties of water on solar altitude. *Limnol. Oceanogr.* **29**: 350–356.
- KRUSE, F. A., A. B. LEFKOFF, J. B. BOARDMAN, K. B. HEIDEBRECHT, A. T. SHAPIRO, P. J. BARLOON, AND A. F. H. GOETZ. 1993. The Spectral Image Processing System (SIPS)—interactive visualization and analysis of imaging spectrometer data. *Remote Sensing Environ.* **44**: 145–163.
- KUTSER, T. 1997. Estimation of water quality in turbid inland and coastal waters by passive optical remote sensing. *Diss. Geophys. Univ. Tartuensis* **8**: 160.
- , H. ARST, S. MÄEKIVI, AND K. KALLASTE. 1998. Estimation of the water quality of the Baltic Sea and lakes in Estonia and Finland by passive optical remote sensing measurements on board vessel. *Lakes Reservoirs Res. Manage.* **3**: 53–66.
- , ———, ———, J.-M. LEPPÄNEN, AND A. BLANCO. 1997. Monitoring algae blooms by optical remote sensing, p. 161–166. *In* A. Spiteri [ed.], *Remote sensing '96*. Balkema.
- , A. G. DEKKER, AND W. SKIRVING. 2003. Modelling spectral discrimination of Great Barrier Reef benthic communities by remote sensing instruments. *Limnol. Oceanogr.* **48**: 497–510.
- , A. HERLEVI, K. KALLIO, AND H. ARST. 2001. A hyperspectral model for interpretation of passive optical remote sensing data from turbid lakes. *Sci. Total Environ.* **268**: 47–58.
- , I. MILLER, AND D. L. B. JUPP. 2002. Mapping coral reef benthic habitat with a hyperspectral space borne sensor. *Proc. Ocean Optics XVI, Santa Fe, 14 pp* (CD-ROM), Office of Naval Research.
- LEPPÄNEN, J.-M., E. RANTAJÄRVI, S. HÄLLFÖRS, M. KRUSKOPF, AND V. LAINE. 1995. Unattended monitoring of potentially toxic phytoplankton species in the Baltic Sea in 1993. *J. Plankton Res.* **17**: 891–902.
- MÄEKIVI, S., AND H. ARST. 1996. Estimation of the concentration of yellow substance in natural waters by beam attenuation coefficient spectra. *Proc. Estonian Acad. Sci. Ecol.* **6**: 108–123.
- MORAN, M. S., R. BRYANT, K. THOME, W. N. Y. NOUVELLON, M. P. GONZALES-DUGO, J. QI, AND T. R. CLARKE. 2001. A refined empirical line approach for reflectance factor retrieval from Landsat-5 TM and Landsat-7 ETM+. *Remote Sensing Environ.* **78**: 71–82.
- PAERL, H. W., AND J. F. USTACH. 1982. Blue-green algal scums: An explanation for their occurrence during freshwater blooms. *Limnol. Oceanogr.* **27**: 212–217.
- PATERSON, D. M., K. H. WILTSHIRE, A. MILES, J. BLACKBURN, I. DAVIDSON, M. G. YATES, S. MCGRORTY, AND J. A. EASTWOOD. 1998. Microbiological mediation of spectral reflectance from intertidal cohesive sediments. *Limnol. Oceanogr.* **43**: 1207–1221.
- PEARLMAN, J. S., P. S. BARRY, C. C. SEGAL, J. SHEPANSKI, D. BE-

- ISO, AND S. L. CARMAN. 2003. Hyperion, a space-based imaging spectrometer. *IEEE Trans. Geosci. Remote Sensing* **41**: 1160–1173.
- PIERSON, D. C., AND N. STRÖMBECK. 2001. Estimation of radiance reflectance and the concentrations of optically active substances in Lake Mälaren, Sweden, based on direct and inverse solutions of a simple model. *Sci. Total Environ.* **268**: 171–188.
- QUIBELL, G. 1992. Estimating chlorophyll concentrations using upwelling radiance from different freshwater algal genera. *Int. J. Remote Sensing* **13**: 2611–2621.
- RANTAJÄRVI, E., R. OLSONEN, S. HÄLLFORS, J.-M. LEPPÄNEN, AND M. RAATEOJA. 1998. Effect of sampling frequency on detection of natural variability in phytoplankton: Unattended high-frequency measurements on board ferries in the Baltic Sea. *ICES J. Mar. Sci.* **55**: 697–704.
- RICHARDSON, L. L. 1996. Remote sensing of algal bloom dynamics. *BioScience* **46**: 492–501.
- SCHALLES, J. F., A. A. GITELSON, Y. Z. YACOBI, AND A. E. KROENKE. 1998. Estimation of chlorophyll *a* from time series measurements of high spectral resolution reflectance in an eutrophic lake. *J. Phycol.* **34**: 383–390.
- SELLNER, K. G. 1997. Physiology, ecology, and toxic properties of marine cyanobacteria blooms. *Limnol. Oceanogr.* **42**: 1089–1104.
- SIEGEL, H., AND M. GERTH. 2000. Remote-sensing studies of the exceptional summer of 1997 in the Baltic Sea: The warmest August of the century, the Oder flood, and phytoplankton blooms, p. 239–255. *In* D. Halpern [ed.], *Satellites, oceanography and society*. Elsevier Science.
- , ———, T. NEUMANN, AND R. DOERFFER. 1999. Case studies on phytoplankton blooms in coastal and open waters of the Baltic Sea using Coastal Zone Colour Scanner data. *Int. J. Remote Sensing* **20**: 1249–1264.
- SMITH, R. C., AND K. S. BAKER. 1981. Optical properties of the clearest natural waters (200–800 nm). *Appl. Optics* **20**: 177–184.
- STRAMSKI, D., A. BRICAUD, AND A. MOREL. 2001. Modelling the inherent optical properties of the ocean based on the detailed composition of the planktonic community. *Appl. Optics* **40**: 2929–2945.
- SVEJKOVSKY, J., AND J. SHANDLEY. 2001. Detection of offshore plankton blooms with AVHRR and SAR imagery. *Int. J. Remote Sensing* **22**: 471–485.
- VINCENT R. K., X. QIN, R. M. L. MCKAY, J. MINER, K. CZAJKOWSKI, J. SAVINO, AND T. BRIDGEMAN. 2004. Phycocyanin detection from LANDSAT TM data for mapping cyanobacterial blooms in Lake Erie. *Remote Sensing Environ.* **89**: 381–392.

*Received: 5 November 2003*

*Accepted: 21 May 2004*

*Amended: 4 June 2004*